Int. J. Nano Dimens., 11 (4): 303-311, Autumn 2020

ORIGINAL ARTICLE

Multi element doped type-II heterostructure assemblies (N, S-TiO_2/ZnO) for electrochemical crystal violet dye degradation

Dilip Kumar Behara*, Devangam Vishnu Priya Alugoti, Palukuru Pooja Sree

Department of Chemical Engineering, JNTUACEA, Ananthapuramu-515002, India

Received 09 May 2020; revised 03 September 2020; accepted 09 September 2020; available online 09 September 2020

Abstract

Herein, we report multi-element doped Type-II heterostructure assembly consists of N, S doped TiO_2 and ZnO for electrochemical crystal violet dye degradation studies. Electrochemical measurements were performed on these synthesized N-S codoped TiO_2/ZnO compositeheterostructured assemblies which are fabricated on Titanium (Ti) substrate. It was observed that a composite electrode (N, S-TiO_2/ZnO@Ti) assembly has shown better efficiency metrics in comparison to all individual electrodes (bare Ti, TiO@Ti, ZnO@Ti) highlighting the importance of heterostructures. The findings of this article will help to design economic materials for complex dye molecule degradation studies as well as paves path towards better understanding of molecular mechanisms of dye degradation.

Keywords: *Crystal Violet Dye; Synergistic Interaction; Type-II heterostructure; TiO2; ZnO.*

How to cite this article

Kumar Behara D., Vishnu Priya Alugoti D., Pooja Sree p. Multi element doped type-II heterostructure assemblies (N, S- TiO2/ ZnO) for electrochemical crystal violet dye degradation . Int. J. Nano Dimens., 2020; 11 (4): 303-311.

INTRODUCTION

Energy and environment are the two main important buzz words in today's research world as both are prerequisites to economic and sustainable development of the country. In contemporary research, wastewater treatment has been given considerable importance due to the immense presence of dyes in various industry outlets creating not only a serious threat to human life but also effecting the global environment. These dyes containing water bodies not only create non-aesthetic pollution but also lead to dangerous by products via different reactions schemes such as oxidation, hydrolysis etc. [1, 2]. Further, some of these dyes are carcinogenic in nature and can cause serious damage to human life [3]. Therefore, it is essential to treat or remove the dyes from wastewater streams to minimize the impact of dyes in polluting the environment [4]. Numerous wastewater treatment methods such as conventional physical, chemical, and biological technologies are widely employed till date [5, 6]. However, they are not only consistent in terms of purity of separation but also expensive. In recent years, electrochemical oxidation processes emerged as best alternative methods for the treatment of wastewater, due to its ease of operation, fast reaction rate and being environmental friendly [7-13]. Further, there are no byproducts formed during this treatment and hence there is no requirement of sludge disposal techniques.

Semiconductors play an important role in electrochemical oxidation techniques and have been widely used for various applications such as water splitting, solar cell and pollutant degradation [14-16]. Among the various semiconductors, TiO_2 and ZnO have received much attention due to their low cost, chemical stability, and impressive photocatalytic performance [17, 18]. However,

* Corresponding Author Email: *dileepbh.chemengg@jntua.ac.in*

both TiO_2 and ZnO suffer from relatively large band gap which impedes thier applications. Therefore, it is essential to overcome this limitation for these materials for effective usage in various applications. However, the absorption coefficient of TiO_2 material will be improved by doping with non metals like nitrogen (N) and sulfur (S) which are *iso*-electronic species equivalent with TiO_2 and hence can be easily occupied into TiO_2 matrix [19-21]. Additionally, the addition of dopants to TiO_2 will not increase the the BET surface area by restraining the crystalline growth of TiO_2 but also increase the percentage of anatase phase [22-23]. Further, doping will fetch to form interstitial sites/ oxygen vacancy sites of TiO_2 lattice and is shown to promote other interesting effects with regard to the electro-catalytic activity of the TiO_2, such as decreasing the electron-hole recombination rate and changingthe kinetics of electron (e^-) or hole (h^+) transfer [24, 25]. It is known that forming composite/heterostructure with suitable band edge material like ZnO will improve the performance due to synergistic interaction as well as synchronized charge transport [26, 27]. Therefore, a composite assembly of TiO_2 and ZnO will improve the performance by forming a Type-II heterostructure [28, 29].

Herein, we propose electrochemical degradation of crystal violet dye using N-S co-doped TiO_2/ZnO composite heterostructured assemblies fabricated on titania (Ti) substrate. Titania substrate is chosen as good support due to its stability, and better conductivity. Since the conduction band (CB) edge of TiO_2 is -4.15eV and that of ZnO is -4.21eV w.r.t. Absolute Vacuum Scale [30], there is a net movement of charge carriers from TiO_2 to ZnO, which break the dye molecule at a faster rate. The fabricated electrodes were characterized using varous surface characterization techniques. Further, to monitor electrochemical activity, analytical techniques such as cyclic voltammetry and UV-Vis spectroscopy measurements were used. The faster rate of decolourization is achieved with N, S-TiO_2/ ZnO electrode (~9hrs) in comparison to individual electrodes. This signifies the importance of *iso*-electronic non- metal (N, S) doped metal oxide Type-II Heterostructure in facilitating the fast charge carrier movements and thereby enhancing the electrochemical performance. The outcomes of the current article will not only give direction in understanding the molecular mechanism of dye degradation but also paves path towards exploration of low-cost catalytic heterostructure assemblies for different catalytic/electro-catalytic applications.

EXPERIMENTAL SECTION

Materials and Methods

Titanium tetraiso-propoxide (TTIP) $[Ti\{OCH(CH_3)_2\}_4]$, zinc nitrate $(Zn(NO_3)_2.6H_2O)$, potassium hydroxide(KOH), ethanol (C_2H_5OH), ammonia(NH_3), thiourea ($(NH_2)_2CS$), sodium sulphate (Na_2SO_4), and isopropyl alcohol (C_3H_8O) purchased from Sigma Aldrich Chemicals (India) Ltd. Nafion (10%) liquid solution is purchased DuPont Chemicals, USA. Crystal violet dye purchased from Sigma-Aldrich is used as a model pollutant in the present study. All the reagents were systematically graded and used as received without further purification. All solutions were prepared with distilled water.

Synthesis of doped/un-doped and co-doped nanoparticles

Proportionate amount fo ethanol (150 ml) and de-ionized water (3.75 ml) of were taken and stirred for half an hour to get a homogenous mixture. Controlled amount (~ 9 ml) of TTIP (titanium tetra iso-propoxide) was added drop by drop to this solution while stirring. Further, the stirring is continued for 4 hrs at 85 ºC. The obtained solution centrifuged at 2000 rpm for 30 min followed by drying and calcination at 400 ºC for 3 hours in a muffle furnace to get TiO_2nanoparticles. Ammonia, thiourea or both were added during the synthesis of TiO_2 to yield the formation of N-TiO_2, S-TiO_2 and N, S-TiO_2 nanoparticles respectively as shown in Fig.1 [24].

Synthesis of ZnOnanoparticles

Zinc Oxide (ZnO) nanoparticles were synthesized via direct precipitation method using zinc nitrate hexa hydrate ($Zn(NO_3)_2.6H_2O$) and potassium hydroxide (KOH) as precursors as shown in Fig.1[31]. An aqueous solution of 0.2 M zinc nitrate hexa hydrate and 0.4 M of potassiumhydroxide solutions were prepared separately. The addition of KOH solution to zinc nitrate solution at room temperature results in the white suspension. Finally, the white product was centrifuged at 5000 rpm for 20 minutes and washed several times times with distilled water and absolute ethanol. The final product was

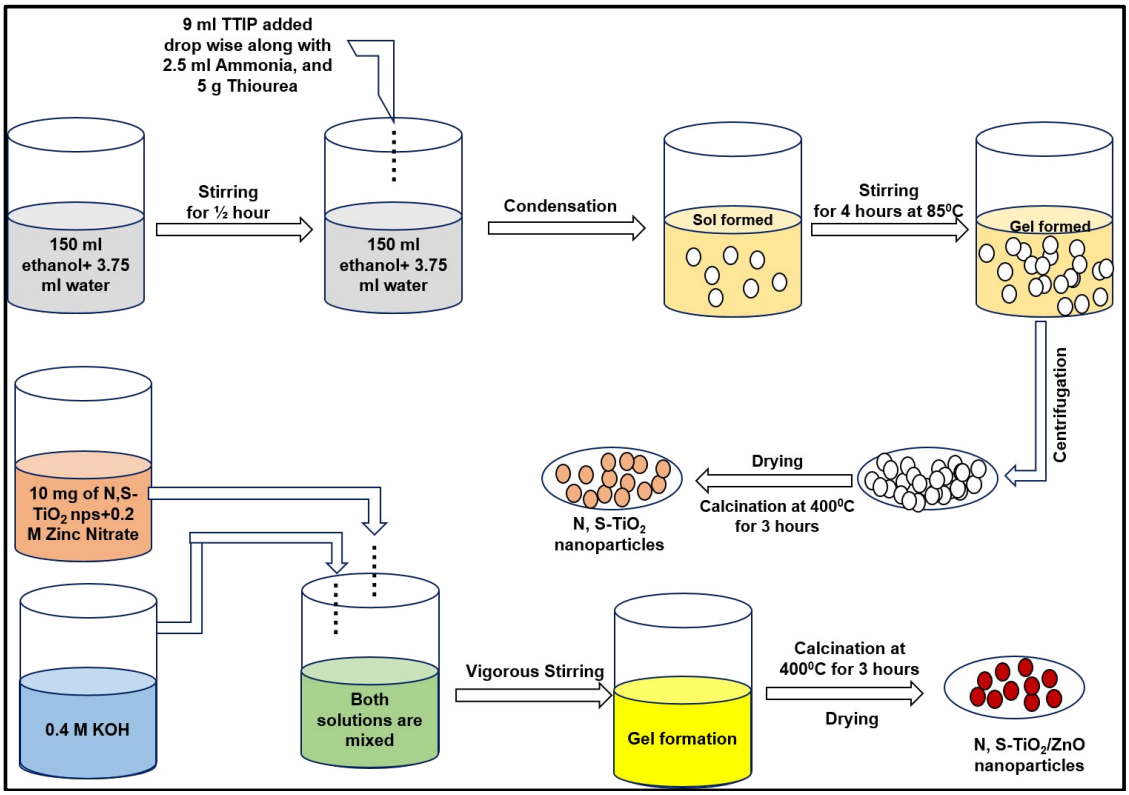

Fig. 1. Schematic representation of synthesis of N, S doped TiO_2, and N, S doped TiO_2/ZnO nanocomposites.

calcined at 500 ºC in an air atmosphere for 3 hours in a muffle furnace to get ZnO nanoparticles.

Synthesis of N, S -TiO_2/ZnOnanocomposite

The synthesis of N, S-TiO_2/ZnOnanocomposite is shown in Fig.1. Approximately 10 mg of nitrogen, sulphur co-doped titanium dioxide (N, S-TiO_2), is added to 0.2 M of zinc nitrate hexa hydrate (Zn $(NO_3)_2.6H_2O$) and 0.4M KOH. To the zinc nitrateand N, S-TiO_2 solutions, KOH solution was slowly added drop wise at room temperature under vigorous stirring and white suspension will be formed which was centrifuged at 5000 rpm for 20 min. The formed product was dried and calcined at 500 ºC for 3 hours to get N, S-TiO_2/ZnO nanocomposites.

Electrode Fabrication

Approximately 40 mg of synthesized TiO_2, N-TiO_2, S-TiO_2, N, S-TiO_2, N, S-TiO_2/ZnO nanoparticles were mixed with 2 ml of isopropanol and 20 µl of Nafion solution. The mixture was and sonicated for 1 hour and the obtained slurry was pasted on the titania (Ti) plate. Later it is dried at 60 ºC on a hot plate to form a uniform surface on Ti substrate (effective electrode surface ~1cm^2). The electrode fabrication is shown in Fig.1* (supplementary information).

Electrochemical Measurements

Cyclic voltammetric(CV) studies were performed by using a potentiostat (K-Lyte 1.0) to monitor crystal violet dye degradation before and after performing electrochemical analysis. Three electrode system measurements were done using silver/slver chloride as reference electrode, platinum mesh as counter and fabricated catalyst assembly as working electrode. Further, crystal violet dye (55 mg/L) with 1M of Na_2SO_4 was used as supporting electrolyte solution for electrochemical measurements.

RESULTS and DISCUSSION

Characterization of Nanoparticles

X-Ray Diffraction Analysis

Crystallography characteristic of synthesized TiO_2 and ZnO was analyzed using X- ray diffractometer (XRD) with Cu K_α radiation (λ = 1.5406 Å). Obtained diffraction spectrum is then

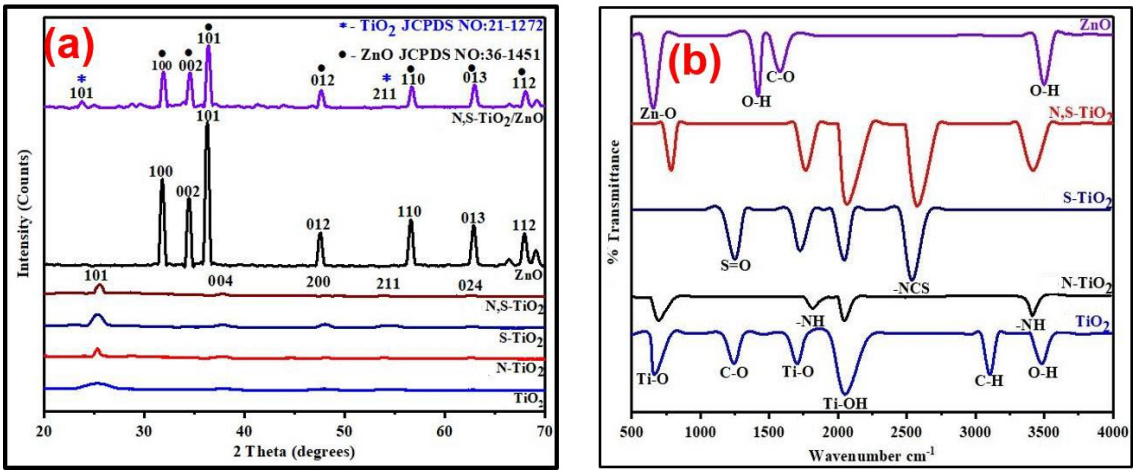

Fig. 2. a) XRD and b) FTIR analysis of pristine and composite samples.

indexed and interpreted by JCPDS data (TiO_2:21-1272, ZnO: 36-1451) [25, 32]. XRD spectra of TiO_2, N-TiO_2, S-TiO_2, N, S-TiO_2, ZnO, and N, S-TiO_2/ZnOnanoparticles were shown in Fig. 2a and Fig 2* (supplementary information). The intense peaks at 2θ values of TiO_2, N-TiO_2, S-TiO_2, N,S-TiO_2 were observed at 25.48˚, 38.72˚, 48.26˚, 55.43˚, 63.22˚ which corresponds to (101), (004), (200), (211), (024) atomic planes respectively confirm the formation of tetragonal Anatase phase matching with JCPDS 21-1272 [24, 25]. The average crystallite size of TiO_2 and ZnO estimated from the Debye-Scherrer formula are 4 and 12 nm respectively. The widening and reduction in internsites of TiO_2 diffraction peaks were observed for doped (N, S) material matrices and implying that reduction in the crystal size and the degree of crystallinity for N-TiO_2, S-TiO_2, N, S-TiO_2 samples as shown in Fig. 2a. Similarly, ZnO exhibits peaks at 31.79º, 34.44º, 36.27º, 47.69º, 57.42º, 63.11º, 68.22º corresponds to 100, 002, 101, 012, 110, 013, 112 indices confirm hexagonal wurtzite structure. Additionally, the composite shows crystalline phase peaks of both N, S-TiO_2andZnO, which confirms the formation of composite (N, S-TiO_2/ZnO). Overall diffraction patterns from XRD patterns indicate the highly crystalline nature of Anatase phase TiO_2, ZnO and N, S-TiO_2/ZnOsamples.

FTIR analysis

The surface functional groups present in the sample can be known from Fourier Transform Infrared Spectroscopy (FTIR). The vibration mode observed at 3483.44 cm^{-1} is attributed to hydroxyl groups (-OH) on the surface of the sample. Further, the transmission band observed at 2029.01 cm^{-1} can be ascribed to the stretching vibration mode surface hydroxyl groups bonded to titanium atoms (Ti-OH). The fundamental crystal lattice vibrations of TiO_2 appear at 665.87 cm^{-1} ascribed to the stretching vibrations of Ti-O bonds as depicted in Fig. 2(b) [33]. The vibrations at 3418.96 cm^{-1} were assigned to N-H stretching, 1854.81 cm^{-1} corresponds to N-H bending which come from N-TiO_2 as depicted in Fig. 2. (black colour) [34]. Similarly, broadband peaks observed at 2782.05 cm^{-1} corresponds to

N=C=S stretching and the peak at 1256.18 $cm^{-1}$are assigned to the asymmetric stretching frequency of S=O bonds of S-TiO_2 [35]. For N, S-TiO_2both N-TiO_2, S-TiO_2 and TiO_2 peaks were obtained (red colour).A peak around 3534.65 cm^{-1} is assigned to the stretching vibration and bending vibration of surface hydroxyl groups on ZnO. The peak at 1568.07 $cm^{-1}$was attributed to the O-C-O stretching vibrations. The peak observed at 1418.84 cm^{-1} is known to be from adsorbed water (bending vibrations). Lastly, the peak at 660.89 cm^{-1} is assigned to ZnO stretching vibrations [31].

SEM, TEM and EDX analysis

Field Emission Scanning Electron Microscopy (FESEM) and Energy Dispersive X-ray Spectroscopy (EDS) were used to determine surface morphology and elemental composition of nanoparticles. From Fig. 3, it is apparent that the surface morphology of the TiO_2 changes with doping of N, S. Basically TiO_2 surface morphology was more or less spherical as depicted in the inset image of Fig. 3(a). Similarly, Zinc Oxide (ZnO) nanoparticles are rod like

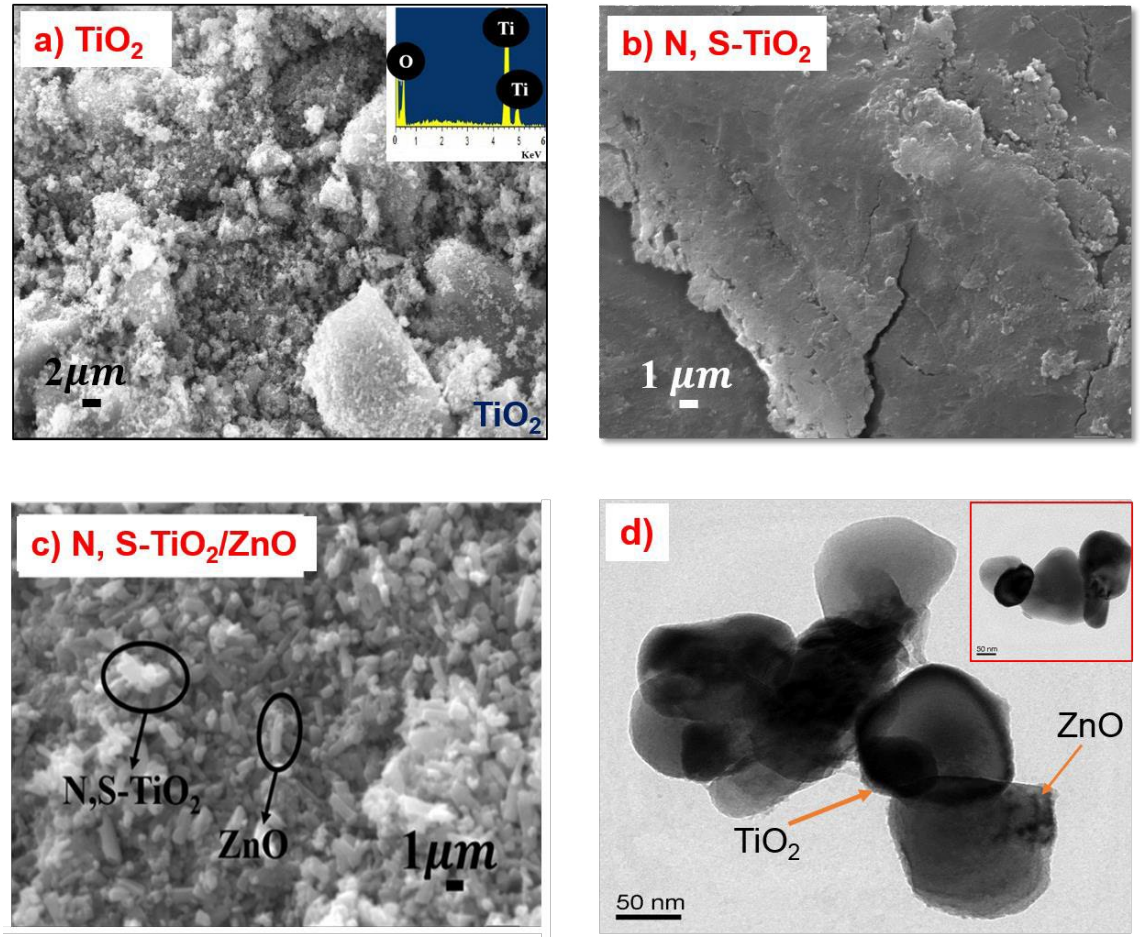

Fig. 3. SEM image of a) TiO_2, b) N, S-TiO_2, c) N, S-TiO_2/ZnO composite, (d) TEM image of N, S-TiO_2/ZnO composite (inset image in 3a shows EDX pattern).

structure at many places with uneven distribution as shown in Fig 3*b(supplementary information). Further, the addition of dopants (N and S) to the crystalline matrix will rupture the surface of TiO_2 and lead to crystal distortion as shown in Fig 3*c, 3*d, and 3*e (supplementary information). The doped samples show the variation of shape that resultsfrom the agglomeration particles of TiO_2 with N, S dopants as shown in Fig. 3(b). EDX usually used to measure the chemical composition of the synthesized nanoparticles. The EDX spectrum of TiO_2 confirms the presence of Ti and O (inset image of Fig 3a). Further, elemental mapping confirms the presence of all elements including dopants (N, S) in all the samples from EDAX spectrum as shown in Fig 4* (supplementary information). Though EDX confirms the elemental mapping as well as the presence of composite sample elements but the surface material distribution is not uniform after doping. It may be probably due to surface segregation of the added dopants, and the lattice was completely distorted which was confirmed from the SEM image (Fig. 3c and Fig 3*f supplementary information). Further, to confirm the formation of composite or Heterostructure of materials, TEM images were taken. Fig 3(d) shows the TEM image of a composite sample with N, S doped TiO_2 and ZnO. It is to be noted that TiO_2nanoparticles are sandwiched between ZnOnanoparticles at many places and the adjacent location of these two nanoparticlesconfirms the formation of nanocomposite/Heterostructure as evident from inset image of Fig 3d.

Cyclic Voltammetry (CV) studies

A potential range of -1.5 V to +1.5 Vwasselected and controlled current density of 0.1 mA/cm^2 was maintained for all electrochemical measurements.

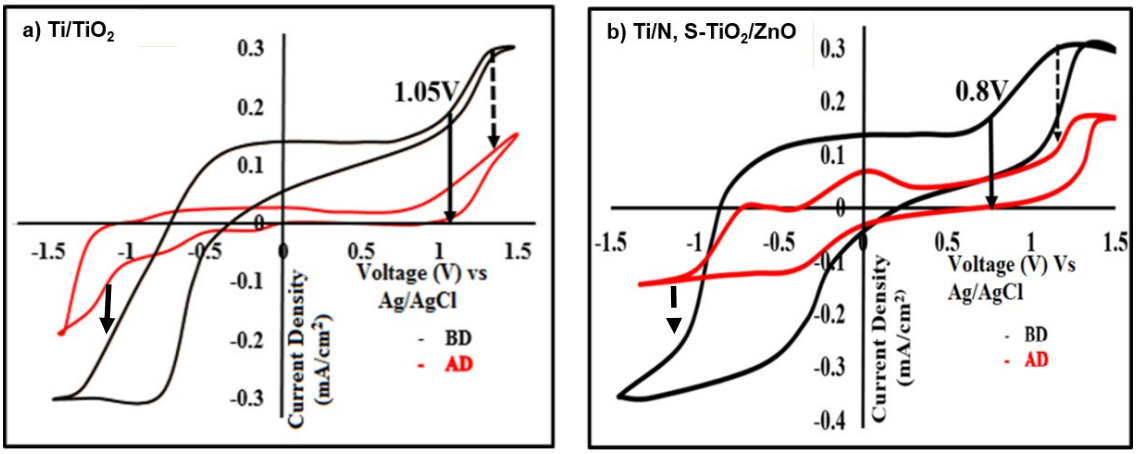

Fig. 4. Cyclic voltammetry(CV) studies for dye degradation at a) Ti/TiO_2, b) N, S- TiO_2/ZnO composite assembly (BDand AD represents Before and after degradation).

- Indicates Voltage where Oxidation Peak Rises - Indicates a Decrease in Peak Current

Cyclic voltammograms exhibit oxidation peak during forward scan and reduction peak during the reverse scan of the electrolysis process. The oxidation peak potential varies for catalyst surface and different samples exhibit different oxidation potentials as shown in Fig 5* (supplementary information).The oxidation of reactive azo groups can be observed by keenly observing the change in currents produced from oxidation and reduction reactions during electrolysis [33]. Further, the absence of peak or reduction in peak will be observed after electrolysis or completion of dye degradation due to complete reduction of chromophoric groups. The electrolyzed solution at this moment was analyzed with HPLC to identify any functional groups present. It is observed that no amino group and no intermediate were detected which indicates the the reactive azo groups were reduced to amines. Fig 4a shows the CV of TiO_2 catalyst fabricated on Ti substrate shows oxidation and reduction peaks at potential of +1.05V and -0.4V respectively. It is understood that if more number of reactive groups are there in dye molecule then it leads to produce more current in CV. Similarly, the decrease in peak current after complete degradation indicates the reduction of reactive groups. The shift in oxidation peak to 0.8V in case of composite assembly N, S-TiO_2/ZnO indicates decolourization of dye and less or non-availability of azo groups in electrolyte solution as shown in Fig 4b. An oxidation peak at 0.8 V is observed for N, S-TiO_2/ZnO samples fabricated on Ti substrate as shown from the voltammogram curve (Fig 4b). Further, the reduction in anodic peaks in CV were observed during electrolysis which indicates the exisiting azo groups were reduced to amines. Additionally, the presence of Na_2SO_4 will favor oxidation of dye by forming persulfate ions. The progress of degradation can be monitored by performing chronoamperometry at a fixed voltage at different time intervals. Chrono-amperometric studies were performed at a fixed voltage (i.e. voltage where oxidation peak rises in CV) 1.2V vs. Ag/AgCl for N, S-TiO_2/ZnO@Ti at a scan rate of 0.05V/s.

Ultra Violet-Visible Spectra analysis

Ultra Violet-Visible Spectra analysis were perfomed to identify the extent of crystal violet dye absorption at different time intervals. The crystal violet dye spectra show an absorbance at 576 nm wavelength. The absorbance in the visible region is attributed to the presence of chromophores (azo) groups. During electrochemical degradation, the aromatic rings as well as –N=N–bonds will break down into small molecules, which results in the decrease of absorbance. The absorption becomes zero at λ_{max}=576 nm indicates the reduction of auxochrome groups. Different electrode assemblies such as Ti/TiO_2, Ti/N-TiO_2, Ti/S-TiO_2, Ti/ZnO, and Ti/N, S-TiO_2/ZnO composite assemblies were used to degrade the crystal violet dye and the decolourization vs. time plots were shown in Fig 6* (supplementary information).The absorbance

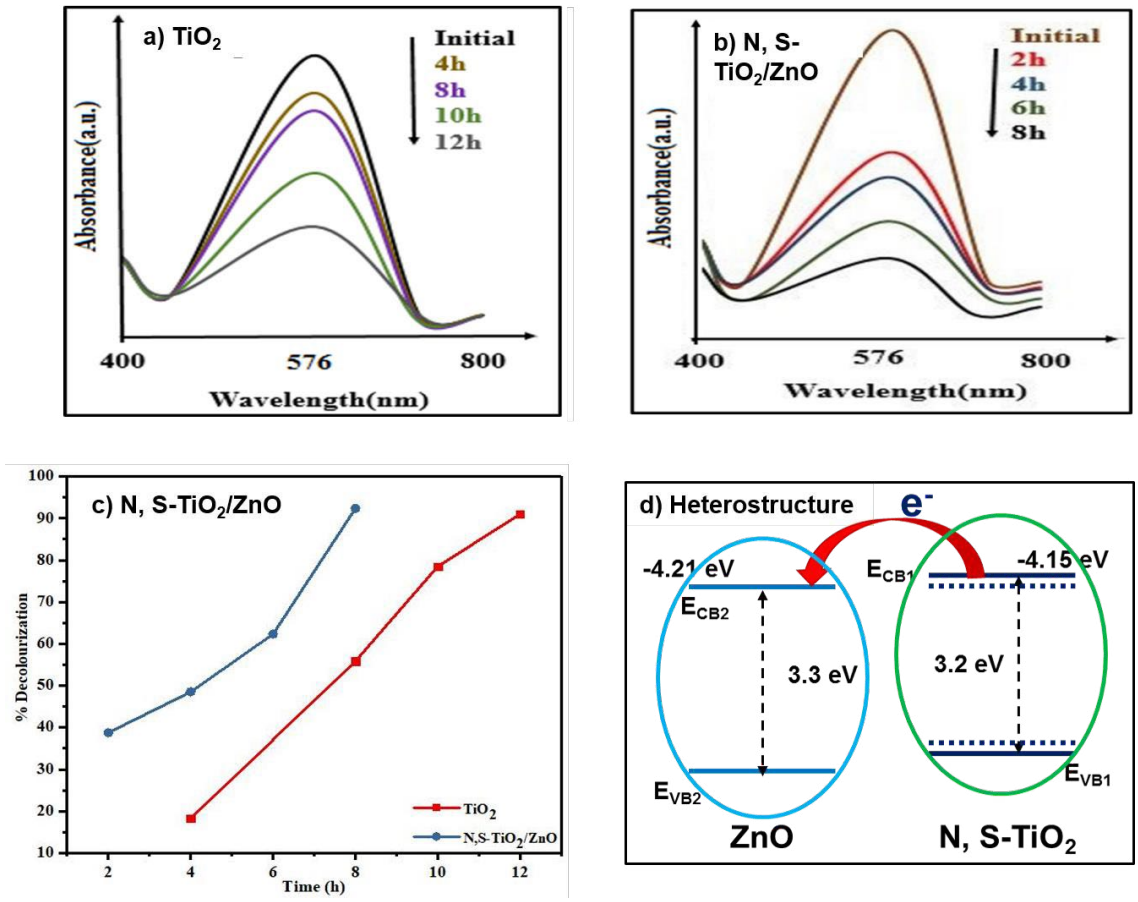

Fig. 5. UV-vis Spectra Analysis a) TiO_2, b) N, S-TiO_2/ZnO composite assembly, c) % decolourization vs. time plot, and d) Type-II Heterostructure band edge alignment showing charge transfer across phases.

Table 1. Time in attaining max % decolorization for various electrode assemblies.

S. No	Name of the electrode assembly	Time in attaining max % decolorization, hrs
1	TiO_2	14
2	N-TiO_2	11
3	S-TiO_2	11
4	ZnO	10
5	N, S-TiO_2	10
6	N, S-TiO_2/ZnO	8

vs wavelength plots for TiO_2 and N, S-TiO_2/ZnO samples were shown in Fig 5a and 5b respectively. A decrease in absorbance with time is observed for both samples and a faster rate of decrease is observed for the composite sample than pristine TiO_2. Further, the decolourization efficiency is calculated by using the following formula.

$$\% \text{ decolourization} = \frac{A_0 - A}{A_0} * 100 \quad (1)$$

Where the absorption of dye solution before and after electrochemical treatment were indicated with at A_0 and A at λ_{max} as shown in Fig. 5c. Complete decolourization (> 90% decolourization) is achieved for all samples at different times by electrochemical treatment. The degradation time is about 14 hr. and 8 hr. for Ti/TiO_2, and Ti/N, S-TiO_2/ZnO respectively as shown in Fig. 5c.The time in attaining max % decolourization for various electrode assemblies was shown in Table 1 for information. The degradation rate varies with varying of electrode assembliesdue

to the change in an electrochemical active surface area (ECSA), which is responsible for adsorption of more dye molecules that interact with oxidizing agents easily [24]. It is observed that Ti/N, S-TiO_2/ZnOnanocomposite showed a faster rate of decolourization compared to Ti/TiO_2 electrode assembly due to the charge carrier flow path available at the interface of semiconductor materials having suitable band edge positions in forming Type-II Heterostructuresas shown in Fig. 5d. [24, 36]. Therefore, doped metal oxides Heterostructureachieve faster degradation compared to individual metal oxides and exemplify the importance of heterostructure assemblies in dye degradation studies. The degradation of crystal violet dye occurs through N- dealkylation process [37] and degradation pathways were well explained in our previously published articles [11, 12].

CONCLUSIONS

Present work aims to understand multi-element doped metal oxide Heterostructures (N, S-TiO_2/ZnO) for electrochemical degradation of crystal violet dye. The synthesized/fabricated electrode assemblies were confirmed using different characterization techniques such as XRD, SEM, TEM, EDS, UV-vis, and FTIR. Experimental results depict that doped heterostructure assembly (N, S-TiO_2/ZnO) degrade crystal violet dye much faster (8 hrs.) than pristine TiO_2 (14 hrs.). Electrochemical measurements show that Ti/N, S-TiO_2/ZnO heterostructured electrode shows better performance of dye degradation (%) in comparison to the all individual electrode assemblies.This can be ascribed may be due to 1) increase in electrochemical active surface area which accommodates more oxidants to interact with dye molecules; 2) increase in electronic conductivity due to appropriate band edges. The results of the current study will help to design low-cost catalytic assemblies in degrading complex dyes of industrial importance.

ACKNOWLEDGEMENTS

The authors wish to thank the Department of Chemical Engineering, JNTUACEA for providing laboratory and powder X-ray diffractometer facilities for XRD analysis. Authors, convey special thanks to D. HimaBindu, for assisting in taking SEM images at IIT BHU. Further, authors wish to acknowledge OTRI-JNTUA and RIPER for providing UV-vis and FTIR characterization of sample analysis.

RESEARCH FUNDING

This work was supported partly from IEI, RandD grant in aid (2016-17) and UGC XII plan funds of JNT University, Ananthapur (AP).

DISCLOSURE STATEMENT

No potential conflict of interest was reported by the authors

REFERENCES

1. Prieto, O., Fermoso, J., Nunez, Y., Del Valle, J. L., andIrusta, R., (2005), Decolouration of textile dyes in wastewaters by photocatalysis with TiO_2. *Sol Energy*. 79: 376-383.
2. Hao, O. J., Kim, H., and Chiang, P. C., (2000),Decolorization of wastewater. *Crit. Rev. Environ.SciTechnol*, 30: 449-505.
3. Afkhami, A., andMoosavi, R., (2010), Adsorptive removal of Congo red, a carcinogenic textile dye, from aqueous solutions by maghemitenanoparticles. *J Hazard Mater.* 174:398-403.
4. Eggen, R. I., Hollender, J., Joss, A., Schärer, M., andStamm, C., (2014),Reducing the discharge of micropollutants in the aquatic environment: the benefits of upgrading wastewater treatment plants. *Environ. Sci. Technol.* 48: 7683-7689.
5. Ahn, D. H., Chang, W. S., and Yoon, T. I., (1999), Dyestuff wastewater treatment using chemical oxidation, physical adsorption and fixed bed biofilm process. *Process Biochem*. 34: 429-439.
6. El-Gohary, F. A., Abou-Elela, S. I., andAly, H. I., (1995), Evaluation of biological technologies for wastewater treatment in the pharmaceutical industry. *Water Sci Technol.* 32:13-20.
7. Comninellis, C., (1994),Electrocatalysis in the electrochemical conversion/combustion of organic pollutants for waste water treatment. *ElectrochimActa*.39: 1857-1862.
8. Martinez-Huitle, C. A., and Ferro, S., (2006),Electrochemical oxidation of organic pollutants for the wastewater treatment: direct and indirect processes. *Chem Soc Rev.* 35:1324-1340.
9. Panizza M., Bocca C., Cerisola G., (2000), Electrochemical treatment of wastewater containing polyaromatic organic pollutants. *Water Res.* 34: 2601-2605.
10. Chen G., (2004), Electrochemical technologies in wastewater treatment. *Sep. Purif. Technol.* 38: 11-41.
11. Behara D. K., Palukuru P. S., Devangam A. V. P., (2020), N, S-codoped TiO_2/Fe_2O_3 heterostructure assemblies for electrochemical degradation of crystal violet dye. *Iran. J. Chem. Chem. Eng.* 39: 171-180.
12. Behara D. K., Mukkara S. M., Jalajakshi T., (2019), TiO_2/Fe_2O_3: Type-I heterostructures for electrochemical dye degradation/water splitting studies. *J. Inst. Eng. India Ser. E*. 100: 189-198.
13. Zhou M., Yu Q., Lei L., Barton G., (2007), Electro-Fenton method for the removal of methyl red in an efficient electrochemical system. *Sep. Purif. Technol.* 57: 380-387.
14. Chen C., Ma W., Zhao J., (2010), Semiconductor-mediated photodegradation of pollutants under visible-light

irradiation. *Chem. Soc. Rev.* 39: 4206-4219.
15. Behara D. K., Upadhyay A. P., Sharma G. P., Kiran B., Sivakumar S., Pala R. G. S., (2015), Heterostructures based on TiO_2 and silicon for solar hydrogen generation. *Adv. Func. Mater.* 219-281.
16. Kamat P. V., (2008), Quantum dot solar cells. Semiconductor nanocrystals as light harvesters. *J. Phys. Chem. C.* 112: 18737-18753.
17. Nagaveni K., Hegde M. S., Ravishankar N., Subbanna G. N., Madras G., (2004), Synthesis and structure of nanocrystalline TiO_2 with lower band gap showing high photocatalytic activity. *Langmuir*. 20: 2900-2907.
18. Lee K. M., Lai C. W., Ngai K. S., Juan J. C., (2016), Recent developments of zinc oxide based photocatalyst in water treatment technology: A review. *Water Res.* 88: 428-448.
19. Umebayashi T., Yamaki T., Itoh H., Asai K., (2002), Band gap narrowing of titanium dioxide by sulfur doping. *Appl. Phys. Lett.* 81: 454-456.
20. Darzi S. J., Mahjoub A. R., Bayat A., (2016), Synthesis and characterization of visible light active S-doped TiO_2 nanophotocatalyst. *Int. J. Nano Dimens. 7:* 33-38.
21. Liu G., Yang H. G., Wang X., Cheng L., Pan J., Lu G. Q., Cheng H. M., (2009), Visible light responsive nitrogen doped anatase TiO_2 sheets with dominant {001} facets derived from TiN. *J. Am. Chem. Soc.* 131: 12868-12869.
22. Devi L. G., Murthy B. N., Kumar S. G., (2010), Photocatalytic activity of TiO_2 doped with Zn^{2+} and V^{5+} transition metal ions: Influence of crystallite size and dopant electronic configuration on photocatalytic activity. *Mater. Sci. Eng. B.* 166: 1-6.
23. Horikawa T., Katoh M., Tomida T., (2008), Preparation and characterization of nitrogen-doped mesoporoustitania with high specific area. *Microp. Mesop. Mater.*110: 397-404.
24. Behara D. K., Ummireddi A. K., Aragonda V., Gupta P. K., Pala R. G. S., Sivakumar S., (2016), Coupled optical absorption, charge carrier separation, and surface electrochemistry in surface disordered/hydrogenated TiO_2 for enhanced PEC water splitting reaction. *Phys. Chem. Chem. Phys*. 18: 8364-8377.
25. Behara D. K., Sharma G. P., Upadhyay A. P., Gyanprakash M., Pala R. G. S., Sivakumar S., (2016), Synchronization of charge carrier separation by tailoring the interface of Si–Au–TiO_2heterostructures via click chemistry for PEC water splitting. *Chem. Eng. Sci.* 154: 150-169.
26. Xiao F. X., (2012), Construction of highly ordered ZnO–TiO_2nanotube arrays (ZnO/TNTs) heterostructure for photocatalytic application. *ACS Appl. Mater. Interfaces.* 4: 7055-7063.
27. Zhang P., Shao C., Li X., Zhang M., Zhang X., Sun Y., Liu Y., (2012), In situ assembly of well-dispersed Au nanoparticles on TiO_2/ZnOnanofibers: A three-way synergistic heterostructure with enhanced photocatalytic activity. *J. Hazard Mater.* 237: 331-338.
28. Guo S., Han S., Mao H., Dong S., Wu C., Jia L., Bo Ch., Li J., (2014), Structurally controlled ZnO/TiO_2 heterostructures as efficient photocatalysts for hydrogen generation from water without noble metals: The role of microporous amorphous/crystalline composite structure. *J. Power Sourc.* 245: 979-985.
29. Lei J. F., Li L. B., Shen X. H., Du K., Ni J., Liu C. J., Li W. S., (2013), Fabrication of ordered ZnO/TiO_2 heterostructures via a templating technique. *Langmuir.* 29: 13975-13981.
30. Wang R., Tan H., Zhao Z., Zhang G., Song L., Dong W., Sun Z., (2014), Stable ZnO@TiO_2 core/shell nanorod arrays with exposed high energy facets for self-cleaning coatings with anti-reflective properties. *J. Mater. Chem. A. Mater.* 2: 7313-7318.
31. Ghorbani, H. R., Parsa Mehr F., Pazoki H., Mosavar Rahmani B., (2015), Synthesis of ZnO nanoparticles by precipitation method. *Orient. J. Chem*. 31: 1219-1221.
32. Al Abdullah K., Awad S., Zaraket J., Salame C., (2017), Synthesis of ZnO nanopowders by using sol-gel and studying their structural and electrical properties at different temperature. *Energy Procedia.* 119: 565-570.
33. Wang C., Hu Q., Huang J., Wu L., Deng Z., Liu Z., Cao Y., (2013), Efficient hydrogen production by photocatalytic water splitting using N-doped TiO_2 film. *Appl. Surf. Sci.* 283: 188-192.
34. Yang G., Jiang Z., Shi H., Xiao T., Yan Z., (2010), Preparation of highly visible-light active N-doped TiO_2 photocatalyst. *J. Mater. Chem.* 20: 5301-5309.
35. Ivanov S., Barylyak A., Besaha K., Bund A., Bobitski Y., Wojnarowska-Nowak R., Yaremchuk I., Kus-Liśkiewicz M., (2016), Synthesis, characterization, and photocatalytic properties of sulfur-and carbon-codoped TiO_2 nanoparticles. *Nanoscale Res. Lett.* 11: 140-147.
36. Gholipour M. R., Dinh C. T., Béland F., Do T. O., (2015), Nanocompositeheterojunctions as sunlight-driven photocatalysts for hydrogen production from water splitting. *Nanoscale*. 7: 8187-8208.
37. Kim C., Kim J. T., Kim K. S., Jeong S., Kim H. Y., Han Y. S., (2009), Immobilization of TiO_2 on an ITO substrate to facilitate the photoelectrochemical degradation of an organic dye pollutant. *Electrochim. Acta.* 54: 5715-5720.